15TH IEA HEAT PUMP CONFERENCE
MAY 26–29, 2026 | HOFBURG
VIENNA 2026
DECARBONISATION THROUGH INNOVATION

Characteristics and optimization of a direct boiling high-temperature steam heat pump

Jie Wang [a, b], Lingxiao Yang [a, b], Zhenqian Chen [a, b *]

[a] Key Laboratory of Energy Thermal Conversion and Control of Ministry of Education, School of Energy and Environment, Southeast University, Nanjing (210000), Jiangsu, PR China

[b] Jiangsu Provincial Key Laboratory of Solar Energy Science and Technology, School of Energy and Environment, Southeast University, Nanjing(210000), Jiangsu, PR China

Abstract

As a conventional steam generation approach in high-temperature steam heat pumps, flash evaporation suffers from several drawbacks, including a complex system configuration, substantial space requirements, and relatively low efficiency. In contrast, direct boiling steam generation offers a more streamlined system architecture and significantly reduces the physical footprint of the installation. It can also narrow the operating condition of the system, thereby enhancing the cycle performance. This study investigates the influence of critical parameters, such as temperature difference and recompression ratio, on the performance of a direct-boiling high-temperature steam heat pump. A mathematical model was developed to investigate the impact of variations in condensing temperature differences and compression ratios on heat capacity and power consumption. The analysis revealed that increasing the condenser temperature difference enhances heat absorption but also raises compressor power consumption, thereby reducing COP. The recompression ratio significantly impacts the temperature distribution within the cycle, with higher ratios increasing superheat and initially improving system COP, which can reach up to a 31.3% enhancement. Optimal recompression ratios are context-dependent, balancing performance, stability, and investment, and are influenced by operating conditions such as saturation steam and environmental heat source temperatures. Within the studied parameters, a recompression ratio of 2.0 to 2.6 is deemed optimal for system efficiency.

Keywords: Steam generating; Recompression; High-temperature heat pump; Performance optimization

1. Introduction

High-temperature steam is widely used in industrial processes, and the low-grade residual heat generated after its application is often not effectively utilised. For a long time, industrial production processes have primarily relied on fossil fuels for heating. In 2030, climate, energy, transport, and tax policies aim to reduce net greenhouse gas emissions by 55 % , as described in the European Green Deal [1]. As a highly efficient and energy-saving heating technology, heat pumps play a pivotal role in energy conservation, emission reduction, and achieving carbon neutrality. Therefore, to fulfil the goal of environmental sustainability as soon as possible, the development of heat pumps has become a research focus [2]. In this background, the development of high-temperature heat pumps for industrial applications holds significant potential and importance [3].

High-temperature heat pump steam systems operate at elevated temperatures during heating cycles and require a greater temperature rise. Currently, high-temperature steam heat pumps primarily consist of two types: flash-type high-temperature heat pumps and two-stage compression heat pumps [4]. The first type involves installing a flash tank directly on the outlet side of the high-temperature, high-pressure hot water line to flash the steam [5]. This requires a higher temperature at the heat pump outlet to generate high-temperature steam. Therefore, the structural design and control methodologies of the system necessitate more stringent criteria to ensure enhanced performance and reliability. Subcooling the working fluid to a certain degree before throttling can effectively enhance system performance[6-7]. Experimental investigations by Shiravi et al. [8]demonstrate that a certain degree of subcooling yields a marked enhancement in both the Coefficient of Performance (COP) and heating capacity of high-temperature heat pump systems. Furthermore, it has been established that both intermediate gas injection and cascade systems represent viable technical pathways for enhancing the

* Corresponding author. *E-mail address:* zqchen@seu.edu.cn (Z. Chen).

performance of high-temperature heat pumps [9-10]. Zou et al. [11] investigated a cascade high-temperature heat pump (HTHP) system with injection, focusing on optimising the stage matching among the heat source temperature, heating temperature, intermediate temperature, and injection pressure. It indicated that under conditions of 20 °C ambient temperature and 130 °C heat supply temperature, an increase in the heating COP to 1.65 is reported for the matched system, representing an 18.71 % enhancement over the unmatched baseline. In summary, research focus has been predominantly centred on enhancing heat pump performance through the incorporation of ancillary components, such as subcoolers and injectors, into standard system architectures.

In contrast to flash heat pump systems, two-stage compression systems incorporate a water vapor compressor at the output end, which can generate high-temperature steam without requiring auxiliary heating equipment. This HTHP system was first developed by Kobe Steel in Japan in 2011, which generates steam at a temperature of 135-175 ℃ [12]. Liu et al. [13] combined vapor compression and absorption to propose a hybrid SGHP system. The experimental research has successfully achieved efficient utilisation of flue gas waste heat to produce process steam exceeding 150 °C. Zhao et al.[14] indicated HTHP systems have higher COP and economic costs without a flash cycle. Yan et al.'s simulation study indicates that an optimal intermediate temperature exists between the high-temperature heat pump cycle and the water vapor compressor [15]. Additionally, some researchers proposed specific operating conditions and optimization strategies for the successful implementation of HTHP [16-17]. The generation of high-temperature steam requires water vapor compressors to meet the demands of high pressure ratios, large volumetric flow rates, and high compression temperatures. The integration of heat pumps with mechanical vapor recompression (MVR) has emerged as a promising pathway to decarbonize steam generation. A prominent example is the AHEAD project in Austria, which demonstrates a cascade system utilizing natural refrigerants to uplift waste heat, successfully achieving steam delivery temperatures of 184 °C for pharmaceutical applications[18].Meanwhile, the performance of water vapor compressors remains a significant barrier, hindered by issues such as lubricant corrosion and water vapor ingress. Further technological advancements in this component are required.

Overall, current research on high-temperature heat pump steam is predominantly based on the flash evaporation of hot water to produce low-pressure steam. The system’s structural complexity, coupled with substantial heat loss during pressure reduction, results in low overall thermal efficiency. The incorporation of a water vapor compressor offers a pathway to superior system performance. However, its compatibility with heat pump cycles still requires further research. Research on heat pump-based direct steam generation (DSG) is relatively scarce. Therefore, to address these research gaps, a novel and efficient Direct Boiling High-Temperature Steam Heat Pump (HTHP) is developed in this investigation. This study investigates the characteristics and performance optimization of a direct-boiling high-temperature steam heat pump system by developing a simulation model that incorporates validated experimental data. The innovations of this investigation are as follows:

(1) Investigation into the Effect of Condensation Temperature Difference and Compression Ratio on System Performance.

(2) The effect of different recompression ratios on both the temperature rise distribution and the overall performance of the system.

(3) The characteristics and optimization of a system under varying saturated steam heating temperatures and ambient waste heat temperatures.

This study offers valuable insights and guidance for enhancing the structural improvement and optimizing the performance of related steam heat pump systems.

2. System description

2.1 System principle

The HTHP primarily comprises an evaporator, steam generator, two-stage compressor, economiser, throttling valve, separator, water supply pump, and steam compressor. The two-stage compression cycle is employed to ensure a reliable operational framework within high-temperature steam heat pump systems. The integration of intermediate gas injection and subcooling enhances key system performance. The purpose of a steam compressor is to increase the upper limit of the steam-generating temperature. To elucidate the working principle, the complete thermodynamic cycle is illustrated in detail. The low-pressure superheated refrigerant (state 1-1’) is compressed by the low-stage compressor to the interstage pressure, where it mixes with the saturated vapor refrigerant at the economizer outlet (state 8-2). The medium-pressure superheated refrigerant (state 1’) is compressed by the high-stage compressor to the condensation pressure (state 3), and then flows into the boiling condenser to release heat. The condensed refrigerant is first subcooled in the economizer (state

4-5) and is then expanded through throttle valve A to form a two-phase flow (state 6). The refrigerant enters the separator, where it separates into saturated vapor (state 7) and saturated liquid (state 9). The separated vapor is superheated in the economizer (state 7-8), while the resulting saturated liquid undergoes secondary expansion through throttle valve B (state 9-10). The throttled refrigerant completes the cycle by absorbing heat and evaporating in the evaporator(state 10-1). Finally, the saturated steam from the boiling condenser is directed to the steam compressor, where it is recompressed into high-temperature steam(state 11-12).The working principles of the HTHP are illustrated in Fig. 1 (a). Detailed information regarding the specific processes and key points integral to the modelling methodology can be referenced in Fig. 1 (b).

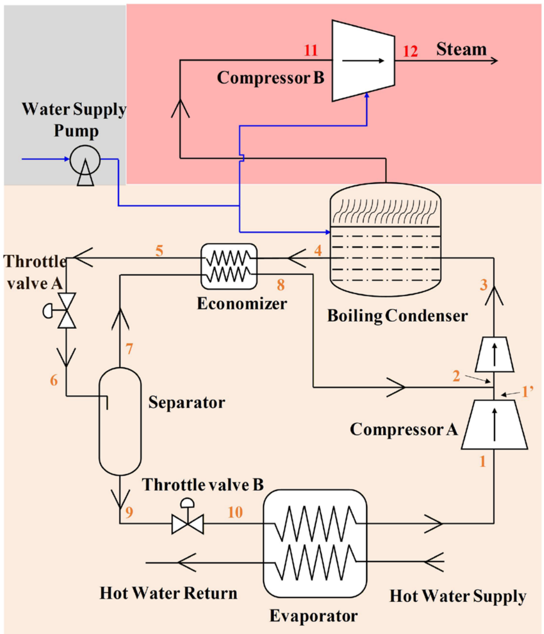

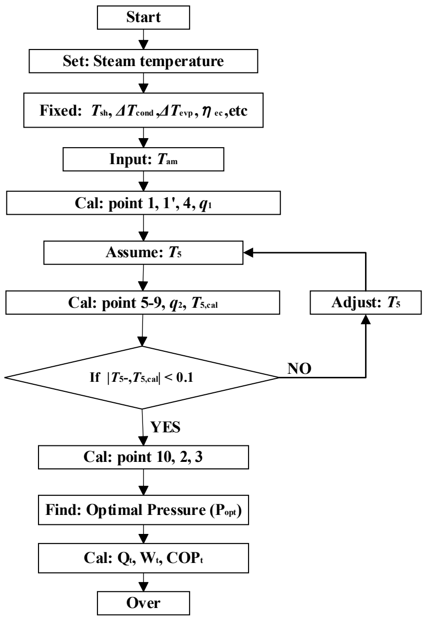

Fig. 1. Description of the HTHP system. (a) Schematic diagram , (b) flowchart for the simulation procedure

2.2 Methodology

This section mainly presents the establishment process of the mathematical models for the heat pump cycles mentioned in Section 2.1. The physical properties of R1233zd(E) and water are calculated by Refprop 10.0.

The specific parameter configurations are detailed in Table 1.

Table 1 Some of the parameter settings for the energy model

Parameters	Values
Superheated degree at evaporator outlet (T_{sh})	5°C
Average evaporator heat transfer temperature difference (ΔT_{evap})	5°C
Average condenser heat transfer temperature difference (ΔT_{cond})	6°C
Mechanical efficiency of the compressor (η_{me})	0.9
Motor efficiency of the compressor (η_{mo})	0.9
Economizer efficiency (η_{ec})	0.7
Compressor displacement (V)	1.3e^{-4} m^3
Compressor speed (n_{com})	1450 rpm

Prior to model development, several simplifying assumptions were introduced to streamline the analysis:

1. The throttling process is considered adiabatic, meaning that the enthalpy remains constant before and after throttling.
2. Heat exchange and pressure drop losses to the outside from other system components and piping are ignored during operation.
3. The separation efficiency of the gas–liquid separator is considered to be 100 %.
4. The system is in steady state during the study.

The mass flowrate at the suction port of the compressor (q_1) can be obtained from Equation (1).

$$q_1 = V \cdot n_{com} \cdot \eta_{vol} \cdot \rho_1 \tag{1}$$

where V is the compressor displacement; n_{com} is the rotational speed of the compressor; η_{vol} is the volumetric efficiency during compression, and can be calculated by the correlation: $\eta_{\mathrm{vol}} = 0.9768 - 0.0921 \cdot CR^{0.714}$; ρ_1 is the suction density of the compressor.

The compression process of the compressor can be regarded as quasi-secondary compression, which is divided into two compression processes. The compression ratio of the first stage ($\mathrm{CR}_{1\sim1'}$) is given by Equation (2).

$$\mathrm{CR}_{1\sim1'} = P_{\mathrm{m}} / P_1 \tag{2}$$

Where P_1 and P_{m} are the suction pressure and the vapor injection pressure of the compressor, respectively.

The specific enthalpy of the refrigerant at the end of the first stage of compression ($h_{1'}$) is given by Equation (3).

$$h_{1'} = (h_{1',is} - h_1) / \eta_{\mathrm{is}} + h_1 \tag{3}$$

where h_1 is the compressor suction specific enthalpy; $h_{1,\mathrm{is}}$ is the outlet specific enthalpy of the first stage of compression under isentropic conditions; and η_{is} the isentropic efficiency of the compressor, which is calculated by the correlation: $\eta_{\mathrm{is}} = 0.9946 - 0.108 \cdot CR^{0.714}$ [19,20].

The compression ratio of the second stage ($\mathrm{CR}_{2\sim3}$) is shown in Equation (4).

$$\mathrm{CR}_{2\sim3} = P_3 / P_{\mathrm{m}} \tag{4}$$

Where P_3 is the discharge pressure of the compressor.

The mass flow rate of the second-stage compression (q_2) consists of two components: the intake mass flow rate (q_1) and the intermediate charge mass flow rate (q_8).

$$q_2 = q_1 + q_8 \tag{5}$$

$$\omega = q_8 / q_2 \tag{6}$$

ω is the injection ratio of the refrigerant.

During the heat transfer process in the economizer, an energy balance exists as shown in Equation (7).

$$h_4 - h_5 = \omega \cdot (h_8 - h_7) \tag{7}$$

Before the second stage compression begins, the refrigerant that has completed the first stage compression is thoroughly mixed with the refrigerant coming from the vapor injection, and the specific enthalpy after mixing (h_2) is calculated by Equation (8) .

$$h_2 = (q_1 \cdot h_{1'} + q_8 \cdot h_8) / q_2 \tag{8}$$

The specific enthalpy at the end of the second stage of compression (h_3) is given by Equation (9).

$$h_3 = (h_{3,\mathrm{is}} - h_2) / q_2 + h_2 \tag{9}$$

where $h_{3,\mathrm{is}}$ is the outlet specific enthalpy of the second stage of compression under isentropic condition.

The power consumption of the first-stage compression, second-stage compression, and total compression for different high-temperature stages is expressed by Equations (10-12).

$$W_{\mathrm{com},1\sim1'} = q_1 \cdot (h_{1'} - h_1) / \eta_{\mathrm{e}} \tag{10}$$

$$W_{\mathrm{com},2-3} = q_2 \cdot (h_3 - h_2) / \eta_{\mathrm{e}} \tag{11}$$

$$W_{\mathrm{com,HP}} = W_{\mathrm{com},1-1'} + W_{\mathrm{com},2-3} \tag{12}$$

where η_{e} is the electrical efficiency of the compressor, comprises both the mechanical efficiency (η_{me}) and the motor efficiency (η_{mo}).

The throttling process is considered an isenthalpic process,which is expressed by Equations (13-14).

$$h_5 = h_6 \tag{13}$$

$$h_9 = h_{10} \tag{14}$$

In the recompression cycle, the compression ratio of the water vapor compressor is given by Equation (15).

$$\mathrm{CR}_{11\sim12} = P_{12} / P_{11} \tag{15}$$

The power consumed by the water vapor compressor is expressed by Equation (16).

$$W_{\mathrm{com,11\text{-}12}} = q_{11} \cdot (h_{12} - h_{11}) / \eta_{\mathrm{e}} \tag{16}$$

The heating by the water vapor compressor is expressed by Equation (17).

$$Q_{\mathrm{recom}} = q_{11} \cdot (h_{12} - h_{11}) \tag{17}$$

The heating capacity of the high-temperature heat pump cycle (Q_h) and the total system heating capacity (Q_t) are expressed by Equations (18-19).

$$Q_h = q_2 \cdot (h_3 - h_4) \tag{18}$$

$$Q_t = Q_h + Q_{recom} \tag{19}$$

The total power consumption of the heat pump is expressed by Equation (20).

$$W_t = W_{recom} + W_{com,HP} \tag{20}$$

Finally, the heating COP of the heat pump cycle is expressed by Equation (21).

$$COP_t = Q_t / W_t \tag{21}$$

2.3 Model validations

The validation of this study was established through rigorous crossverification with prior experimental research. The base HTHP model was corroborated by comparing its performance metrics with those reported in existing literature. Specifically, under identical operating conditions (T_{am} = 65 ◦C, T_{cond} = 108 ◦C) and using the refrigerant R245fa, the COP value obtained in this study (3.591) exhibited a deviation of 3.53 % from the value documented in Ref. [21] (3.631). This close alignment between the predictions and the literature-verified data confirms the accuracy of the base HTHP cycle model.

Additionally, the heat pump cycle with supercooling and charge compensation is validated as evidenced by References [7] and [11], which investigated systems with supercooled charge and optimized the key parameter of intermediate pressure. As illustrated in Table 2, the performance metrics derived in this study showed deviations of 1.51 % and 7.14 % relative to the values reported in references [11] and [7], respectively. These errors fall within the acceptable range of experimental variation, indicating the reliability of the study.

Table 2 Model validation with existing work

System type	COP	Relative error
B-S cycle	3.759 (Present work)	3.53 %
	3.631 (Existing work) [21]	
Vapor injection cycle with subcooling (I)	1.627 (Present work)	1.51 %
	1.652 (Existing work) [11]	
Vapor injection cycle with subcooling (II)	1.977 (Present work)	7.14 %
	2.129 (Existing work) [7]	

3 . Results and Discussion

After establishing and verifying the heat pump system, a series of interesting and meaningful analyses and calculations are performed. In the HTHP cycle and recompression process, the heat transfer temperature difference and recompression ratio are two critical characteristic parameters; in the HTHP cycle, the degree of subcooling of the refrigerant at the condenser outlet becomes the primary object for investigation and comparative analysis. Through in-depth research of these parameters, this study provides a theoretical basis and analytical foundation for subsequent work.

3.1 Effects of Condensation Temperature Difference and Recompression Ratio on System Performance

The temperature difference in the condenser heat transfer represents a critical parameter influencing the performance of heat pump systems. A large temperature difference during heat transfer can substantially degrade the overall efficiency and operational performance of the heat pump. Fig. 2 illustrates the effect of varied condenser temperature differentials on system performance and cycle power consumption. As shown in the figure, an increase in the temperature differential results in a rise in power consumption and a decline in system performance. Specifically, for every 3 °C increase in the heat transfer temperature difference, the cycle power consumption rises by approximately 15 kW, while the COP decreases by 4 % to 6 %, respectively. Moreover, the circulation power consumption exhibits a positive correlation with the saturation temperature of the generated water vapor under a fixed heat transfer temperature difference, with an incremental rate of approximately 20 % per 10 °C rise. This phenomenon occurs because an elevated saturated vapor temperature raises the system’s evaporation pressure. To maintain the specified heat transfer temperature difference, the compressor is forced to operate at a higher discharge pressure. This increases the compression ratio, resulting in greater power consumption. A comprehensive analysis confirms that an increased condensing temperature difference directly contributes to higher compressor power consumption, thereby impairing the performance of the heat pump cycle. However, a minimal temperature difference can lead to insufficient heat absorption by the cooling medium, resulting in a failure to achieve the desired temperature rise. This inadequate thermal response poses significant challenges for precise system control and stability. Based on a comprehensive consideration of the above factors and existing research [22], the temperature difference for heat transfer in the heat pump cycle for this study has been set at 6 °C.

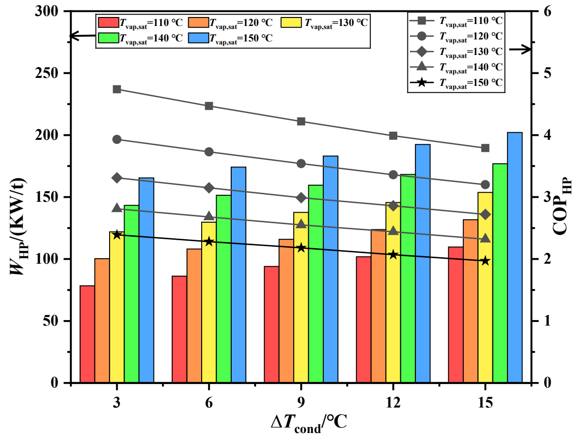

Fig. 2. Effect of ΔT_{cond} on the COP_{HP} and W_{HP} of HTHP cycles

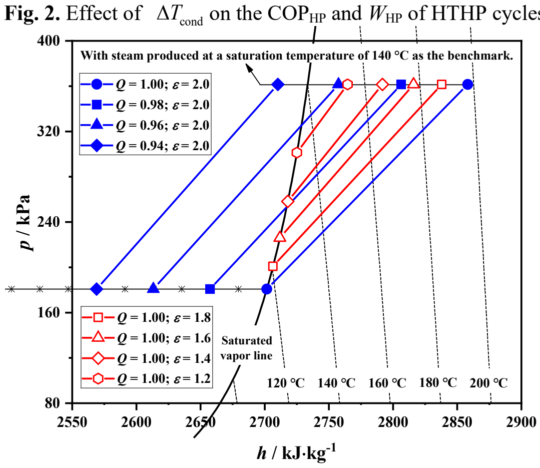

Fig. 3. Effect of compression ratio and dryness fraction on water vapor recompression process

In the recompression process, the magnitude of the compression ratio directly determines the proportion of the temperature rise attributable to the steam compressor. The effect of the recompression ratio (ε_{re}) on the water vapor recompression process is analysed, and the corresponding p-h diagram is given in Fig. 3. This study employs saturated steam at 140 °C (P = 362 kPa) as the baseline, with the compressor output held constant at this state regardless of changes in the recompression ratio. Therefore, the recompression ratio directly influences the compressor's suction pressure. As shown in Fig. 3, an increase in the recompression ratio from 1.2 to 2.0 is inversely related to the suction pressure, which decreases from 301 kPa to 181 kPa, and is accompanied by a rise in the compressor outlet superheat from 14 °C to 58 °C. Therefore, the properties of water vapor dictate that the compression ratio is a critical determinant of the outlet superheat degree in this recompression process. The design of steam recompression cycles typically avoids strict separation measures to prevent unnecessary pressure drops. Consequently, the inlet steam to the water vapor compressor invariably contains a fraction of entrained liquid phase. Furthermore, Fig. 3 illustrates the effect of inlet dryness (Q) on the water vapor recompression process. At a constant compression ratio, the superheat at the compressor outlet decreases significantly as the inlet dryness decreases. It can be demonstrated that the superheat at the compressor outlet can be theoretically lowered through the adjustment of the intake air dryness. Nevertheless, two critical aspects require further consideration. First, the minimum dryness fraction (Q) must be maintained to prevent the outlet superheat from dropping to zero, which could cause wet vapor conditions and potentially lead to liquid ingress and damage to the compressor. Secondly, the direct regulation of the dryness fraction (Q) proves challenging to control with precision. Consequently, intermediate water injection is more effective in practical applications as a method for superheat control. Based on the above analysis, a dryness fraction of 99 % at the compressor outlet is adopted as the baseline parameter for the subsequent investigations.

3.2 Effects of Recompression on System Characteristics and Performance

As shown in Fig. 4, the temperature rise of saturated water vapor during compression can be characterized by the recompression ratio. This study utilizes a 70 °C residual heat source to generate saturated steam at 140 °C, with the base case defined by these operating conditions. Fig. 4 illustrates the electrical energy consumption and heat output per ton of steam as a function of the compression ratio. The total system heat output is attributed to the work input of the heat pump cycle and the ancillary heat associated with vapor compression, which can be calculated using Equation (19). The total power consumption and heating capacity of the system are defined as the sum of the individual contributions from the heat pump cycle and the water vapor compressor, as expressed in Equations (19) and (20), respectively. As illustrated in Fig. 4, the heating capacity of the system demonstrates a significant positive correlation with the recompression ratio. In contrast, the system power consumption remains relatively stable across variations in the recompression ratio, exhibiting an overall trend characterized by an initial slight decrease followed by a gradual increase. Furthermore, an increase in the recompression ratio leads to a significant change in the power consumption ratio between the high-temperature heat pump cycle and the recompression cycle. Research results indicate that the power consumption share of the recompression cycle is susceptible to the compression ratio. Specifically, it increases dramatically from 25 % to 67 % as the compression ratio rises from 1.5 to 6. Therefore, the recompression ratio is the pivotal parameter governing the temperature rise in a water vapor compressor, which is directly proportional to the unit's power consumption. Under a constant overall temperature rise, increasing the share of the temperature rise allocated to the water vapour compressor can reduce the thermal load on the heat pump cycle, thereby effectively enhancing its operational performance. At modest recompression ratios, the performance enhancement attributable to the water vapor compressor is sufficient to justify its additional power consumption within the heat pump cycle. Overall, the recompression ratio serves as a pivotal control parameter, effectively modulating the distribution of temperature rise between the heat pump cycle and the water vapour compressor. The corresponding temperature rise characteristics, along with their underlying mechanisms, will be systematically elucidated in subsequent investigations.

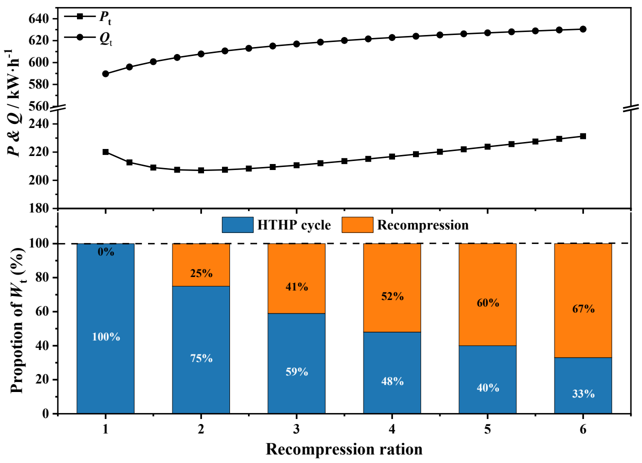

Fig. 4. Effect of Recompression Ratio on System of electricity and Heating Capacity

Fig. 5 illustrates the effect of varying recompression ratios on the overall system performance (COP_t). As shown in Fig. 5, the system exhibits a three-stage variation pattern with an increasing recompression ratio. Initially, the COP_t increases sharply as the recompression ratio rises. Subsequently, the growth rate decelerates and gradually approaches a maximum value. Finally, the COP_t transitions into a regime of gradual decline. To objectively evaluate the impact of compression ratio on system performance, this paper analyzes the issue from two dimensions. On one hand, introducing a recompression process can significantly enhance system operational performance; when the recompression ratio reaches 4.0, the COP_t can increase by up to 22.64 %. On the other hand, optimization focused solely on performance gains has limitations; it is also necessary to comprehensively consider other key influencing factors. After the initial rapid rise, further increase in the recompression ratio results in a marginal gain in the COP_t but a substantial rise in the superheat of the compressor outlet vapor. With the increase in the recompression ratio from 1.0 to 2.5, the COP_t increased by 20.15 %, while the corresponding outlet temperature of water vapor reached 205.7 °C. When the recompression ratio increases to 4.0, the COP_t reaches its peak, but it only improves by 2.49 % compared to when the recompression ratio is 2.5. At the same time, the outlet temperature of the recompression steam also significantly rises to 254.5 °C. When the recompression ratio is increased to 4.0, it attains its maximum.

However, this represents only a modest 1.90 % improvement over the case with a ratio of 2.5, while concurrently resulting in a significant rise in the recompression steam outlet temperature to 254.5 °C. Currently, conventional water vapor compressors typically have an operating temperature limit of 250 °C and can achieve a single-stage compression ratio ranging from 1.0 to 3.027 [22]. Therefore, achieving a compression ratio of 4.0 requires a two-stage water vapor compression system, which results in increased equipment investment costs. In summary, while the introduction of recompression can significantly enhance system performance, selecting the appropriate recompression ratio requires striking a balance between performance gains, operational stability, and capital investment.

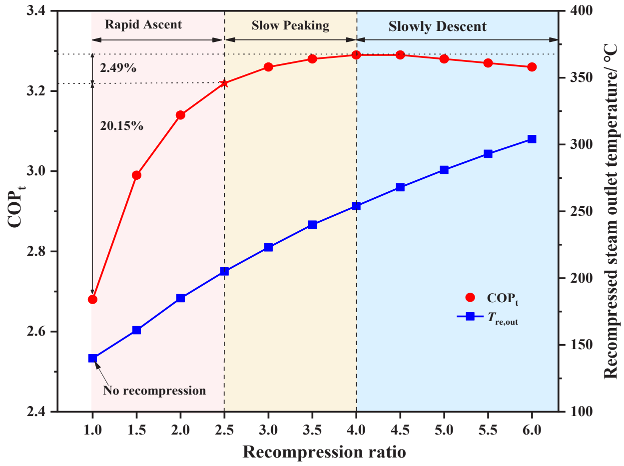

Fig. 5. Effect of Recompression Ratio on Overall System Performance

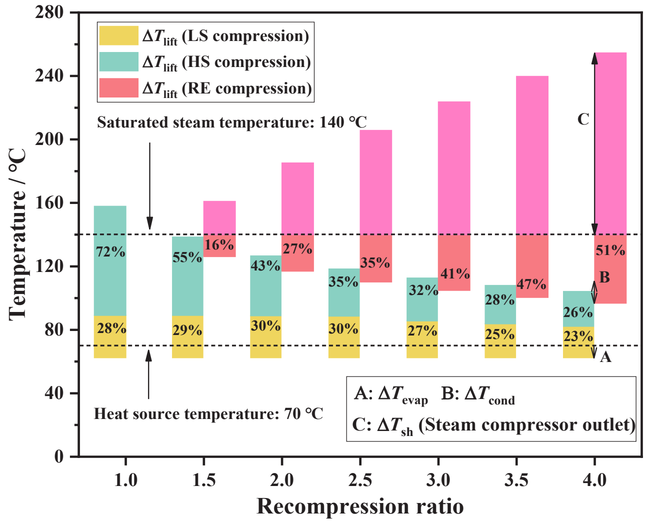

Fig. 6. The Effect of Recompression Ratio on System Temperature Rise Distribution

Fig. 6 presents a relatively novel visualization that intuitively illustrates the influence of different recompression ratios on the overall temperature rise distribution within the system. This chart illustrates how the total temperature rise is achieved. The temperatures associated with the first and second stages of the working medium R1233zd(E) heat pump cycle are indicated by the heights of the yellow and cyan regions, respectively. The additional temperature rise supplied by the water vapor compressor (with water as the working medium) is represented by the adjacent orange region. As indicated in the figure, the parameters A, B, and C are defined as the temperature difference across the evaporator, the temperature difference across the condenser, and the superheat of the steam discharged from the compressor, respectively. As shown in Fig. 6, an increase in the recompression ratio leads to a corresponding increase in the proportion of the temperature rise handled by the steam compressor, accompanied by a significant rise in its outlet superheat. As the recompression ratio increased from 1.5 to 4.0, a substantial shift in thermal load was observed. The compressor's share of the total temperature rise escalated to 51 %, compared to 16 % at the lower ratio, and the outlet steam superheat increased dramatically from 21.6 °C to 114.5 °C. The elevated superheating of water vapor resulting from a higher compressor compression ratio presents a challenge that can be effectively addressed by employing an intermediate water injection strategy. Furthermore, under optimal operating conditions, the temperature rise induced by the first-stage compression is consistently and markedly lower than that of the second stage. This is primarily attributed to the lower suction pressure at the evaporator side of the first-stage compressor.

3.3 Optimization and Matching of System Temperature Rise under Variable Operating Conditions

Fig. 7 illustrates the effect of the saturated steam temperature ($T_{vap,sat}$), varied at 120, 130, 140, and 150 °C, on the performance of the recompression high-temperature heat pump system. The ambient heat source temperature (T_{am}) was maintained at a constant 70 °C in this study. It can be observed from Fig. 7 that the implementation of recompression markedly enhanced the system's performance across all tested $T_{vap,sat}$ levels. As illustrated in Fig. 7, the COP_t of the system across all $T_{vap,sat}$ levels exhibited a consistent three-phase variation pattern. Nevertheless, as the required $T_{vap,sat}$ increases, the optimal recompression ratio to achieve the maximum performance enhancement also rises in tandem. When the $T_{vap,sat}$ is 150 °C, the recompression system demonstrated the most significant performance improvement compared to the baseline system with a compression ratio of 1, exhibiting a coefficient of performance (COP_t) increase of 0.713 in absolute terms, which corresponds to a substantial relative enhancement of 31.27 %. Correspondingly, the system achieved a recompression ratio of approximately 5.0 and a notably high water vapor outlet temperature of 291.9 °C. Therefore, to ensure operational stability and manage investment costs, it is imperative to control the compression ratio of the recompression process, thereby limiting excessively high steam outlet temperatures. In response to the characteristic of the system COP_t , which increases rapidly initially and then plateaus, this study defines the performance gain up to 80 % as "effective gain". In comparison, the subsequent 20 % of the slow increase is considered "marginal gain". Based on this delineation, the system can achieve a substantial reduction in the recompression ratio by sacrificing this marginal gain. At a saturated steam temperature ($T_{vap,sat}$) of 150 °C, increasing the recompression ratio from 1.00 to 2.30 accounted for 80 % of the total 24.74 % performance gain, whereas a further increase to 5.00 provided only a marginal 20 % improvement due to significantly diminishing returns. Fig. 7 presents the optimal effective recompression ratio ($\varepsilon_{re,eff}$) identified in this study, along with the resultant performance enhancement. As the saturated steam temperature ($T_{vap,sat}$) increases from 120 °C to 150 °C, the optimal effective recompression ratio ($\varepsilon_{re,eff}$) rises from 1.95 to 2.30, accompanied by a significant rise in the system's effective lift ratio from 9.84 % to 24.74 %. Consequently, as the required saturated steam temperature increases, both the optimal recompression ratio and the magnitude of performance improvement exhibit an upward trend. This phenomenon is primarily ascribed to the expansion of the system's operational range and the decrease in the baseline COP_t value.

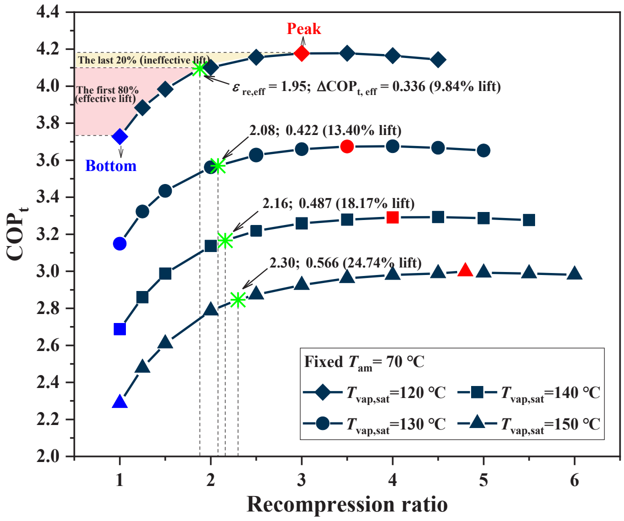

Fig. 7. Analysis and optimization of system characteristics under variable saturated steam temperatures

Fig. 8 further illustrates the impact of varying the ambient heat source temperature (T_{am}) from 50 to 80 °C in increments of 10 °C on the system performance, while the saturated steam temperature ($T_{vap,sat}$) was held constant at 140 °C. As shown in Fig. 8, the system's COP_t at different T_{am} levels follows the same three-stage pattern as that observed in Fig. 8. As the T_{am} increases, the recompression ratio required to achieve the maximum enhancement decreases. When the T_{am} is lowered to 50 °C, the optimum value of COP_t is achieved at a recompression ratio of 5.50. Given that the COP_t system exhibits an initial rapid increase followed by a plateau, performance improvements within the first 80% are defined as "effective gain." In comparison, the subsequent 20 % of gradual growth is categorized as "marginal gain." For the operating condition with a T_{am} of 50 °C, the optimal recompression ratio was determined to be 2.5, which is significantly lower than the peak value of 5.50. Based on this criterion for selecting the optimal recompression ratio, the the optimal effective recompression ratio ($\varepsilon_{re,eff}$) for the four Temperature conditions at 50 °C, 60 °C, 70 °C, and 80 °C are determined to be 2.02, 2.2, 2.35, and 2.5, respectively, with corresponding effective improvement ratios of 21.04 %, 18.47 %, 16.48 %, and 15.71 %. The results indicate that the optimal recompression ratio decreases as the temperature of the heat source increases, accompanied by a marked improvement in system performance.

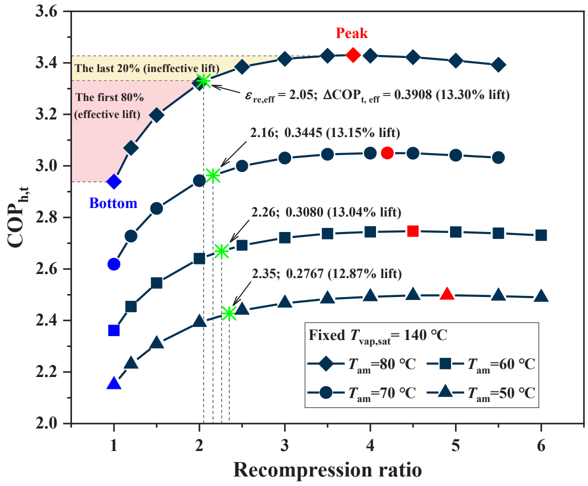

Fig. 8. Analysis and optimization of system characteristics under variable ambient temperatures

Fig. 9 visually demonstrates the temperature rise matching optimization of the system under varying operating conditions, which involves the four sets of conditions studied in Figures 7 and 8. The thermal rise matching optimization in this study is reflected in the following two aspects: Firstly, the intermediate injection pressure of the two-stage compression high-temperature heat pump cycle was optimized through relevant programming, thereby achieving thermal rise matching within the high-temperature heat pump cycle. Secondly, by setting an appropriate recompression ratio criterion, the thermal rise matching of the entire recompression vapor heat pump system was further optimized. Fig. 9 shows that as the system's operating range expands, the temperature rise across all three stages increases, with the second stage (high-temperature stage) of the heat pump cycle consistently playing the dominant role. Furthermore, an increase in both $T_{vap,sat}$ and T_{am} results in a higher temperature rise ratio for the recompression process, as the proportion undertaken by the high-temperature heat pump cycle is reduced. A key finding is that an increase in $T_{vap,sat}$ expands the system's operating range in terms of temperature difference, whereas a decrease in T_{am} broadens the overall operating range. Consequently, while a higher environmental heat source temperature reduces the optimal recompression ratio, the share of the temperature rise allocated to this process rises instead. Generally, the optimal recompression ratio of the system increases as the operating temperature range widens. Meanwhile, the proportion of the temperature rise handled by the recompression process rises with the increase in both the saturated steam temperature and the ambient temperature.

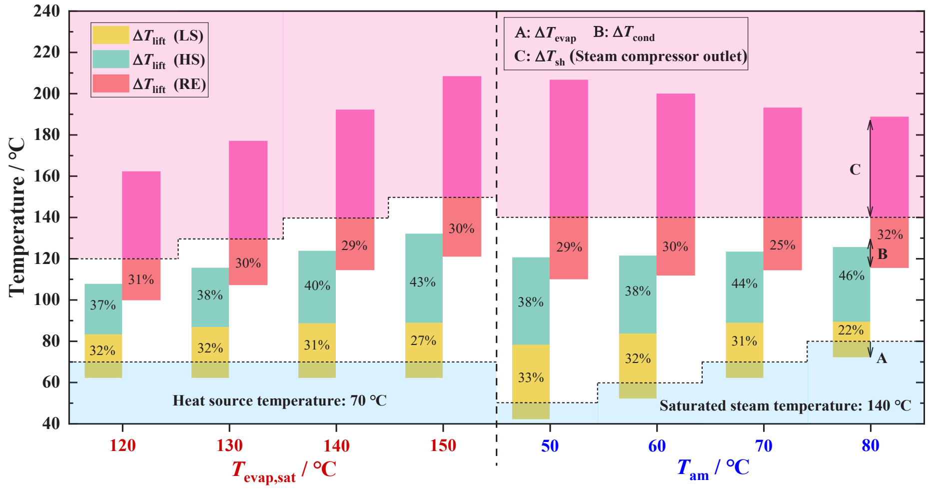

Fig. 9. Optimizing Temperature Rise Matching Under Variable Operating Conditions

4. Conclusion

The focus of the present study is to investigate the effects of critical parameters, including temperature and compression ratio, on a direct-boiling high-temperature steam heat pump and quantify their impact on system efficiency. Firstly, a mathematical model for the high-temperature heat pump was developed to investigate the influence of varying condensing temperature differences and compression ratios on both the heat capacity and power consumption. Furthermore, a performance analysis was conducted based on waste heat and heating temperatures to elucidate the influence of different temperature levels on system performance. The following conclusions can be drawn in this study:

(1) An increased condenser temperature difference elevates compressor power consumption and reduces COP, thereby degrading system performance. However, a minimal difference risks insufficient heat absorption.

(2) The recompression ratio serves as a key variable reflecting the distribution of the temperature rise between the heat pump cycle and the steam compressor. As this ratio increases, the compressor assumes a greater share of the total temperature lift, thereby significantly elevating the degree of superheat at its outlet.

(3) With an increase in the recompression ratio, the system's COP_t initially rises rapidly, then peaks gradually, and finally enters a slow decline. The introduction of recompression significantly enhances system performance, with the maximum COP_t improvement reaching 31.3 % in this study.

(4) An optimal trade-off in compression ratio selection must be struck among system performance, operational stability, and capital investment. The optimal recompression ratio increases with rising saturation steam heating temperatures and decreases with falling environmental heat source temperatures. Within the scope of this study (environmental heat source temperature: 50-80 °C ; saturation steam heating temperature: 120-150 °C), a reasonable recompression ratio falls within the range of 2.0 to 2.6.

(5) Future work will focus on the integration of experiments and simulations for novel working fluids, as well as multi-parameter model validation to enhance reliability. These efforts aim to provide control strategies that are precisely tailored to practical application scenarios.

Nomenclature

COP	coefficient of performance	Subscripts	
HP	heat pump	am	ambient
HT	high-temperature	c	cooling
CR	compressor ratio	cal	calculation
W	power consumption	cond	condensation
Q	heating capacity	com	compressor
P	pressure	ec	economizer
T	Celsius temperature	emiss	emission
ω	dryness	evap	evaporation
η	efficiency	h	heating
V	volumetric flowrate	is	isentropic
q	mass flowrate	m	intermediate
n	compressor speed	is	isentropic
ρ	density	me	mechanical
Δ	difference	mo	motor
W	power consumption	opt	optimal
Q	heating capacity	q	quality
P	pressure	sc	subcooling
T	Celsius temperature	sh	superheating
Δ	difference	t	total
W	power consumption	vol	volume
Q	heating capacity	1-12	state point

Acknowledgements

This work was supported by the National Key Technologies Research and Development Program of China (Grant No. 2024YFB4007400).

References

[1] Communication from the Commission to the European Parliamen[Z].

[2] Ganesan P, Eikevik T M. New zeotropic CO2-based refrigerant mixtures for cascade high-temperature heat pump to reach heat sink temperature up to 180 °C[J]. Energy Conversion and Management: X, 2023, 20: 100407.
[3] Wu W, Du Y, Qian H, et al. Enhancing the waste heat utilization of industrial park: A heat pump-centric network integration approach for multiple heat sources and users[J]. Energy Conversion and Management, 2024, 306: 118306.
[4] Klute S, Budt M, Van Beek M, et al. Steam generating heat pumps – Overview, classification, economics, and basic modeling principles[J]. Energy Conversion and Management, 2024, 299: 117882.
[5] Ma D, Chen Q, Yan G. Thermodynamic and economic analysis of a solar-assisted ejector-enhanced flash tank vapor injection heat pump cycle with dual evaporators[J]. Renewable Energy, 2024, 235: 121368.
[6] Yang L. Characteristic analysis and performance optimization of a transcritical CO2 heat pump for high-temperature heating: An experimental study[J]. 2024.
[7] Dong Y, Yan H, Wang R. Significant thermal upgrade via cascade high temperature heat pump with low GWP working fluids[J]. Renewable and Sustainable Energy Reviews, 2024, 190: 114072.
[8] Ma X, Du Y, Lei B, et al. Energy, exergy, economic, and environmental analysis of a high-temperature heat pump steam system[J]. International Journal of Refrigeration, 2024, 160: 423-436.
[9] Yang L, Wang X, Xu B, et al. Operating characterization and performance optimization of high-temperature heat pumps: A comparative energy, economic and environmental analysis[J]. Applied Thermal Engineering, 2024, 257: 124292.
[10] Dai B, Li X, Liu X, et al. Multi-stage liquid separation condensation high-temperature heat pump system using zeotropic working fluid: System construction and comparison with traditional solutions[J]. Energy, 2025, 330: 136850.
[11] Zou H, Li X, Tang M, et al. Temperature stage matching and experimental investigation of high-temperature cascade heat pump with vapor injection[J]. Energy, 2020, 212: 118734.
[12] Kaida T, Sakuraba I, Hashimoto K, et al. Experimental performance evaluation of heat pump-based steam supply system[J]. IOP Conference Series: Materials Science and Engineering, 2015, 90: 012076.
[13] Liu C, Han W, Xue X. Experimental investigation of a high-temperature heat pump for industrial steam production[J]. Applied Energy, 2022, 312: 118719.
[14] Zhao Z, Yuan H, Gao S, et al. Comparative study on performance and applicability of high temperature water steam producing systems with waste heat recovery[J]. Case Studies in Thermal Engineering, 2021, 28: 101622.
[15] Xu P, Zhang Z, Peng X, et al. Energy, exergy and economic analysis of a vacuum belt drying system integrated with mechanical vapor recompression (MVR) for aqueous extracts drying[J]. International Journal of Refrigeration, 2023, 145: 96-104.
[16] Jin X, Zhang J, Liu Z, et al. Performance analysis of a two-stage vapor compression heat pump based on intercooling effect[J]. Case Studies in Thermal Engineering, 2023, 51: 103643.
[17] Li T, Yang C, Tantikhajorngosol P, et al. Comparative desorption energy consumption of post-combustion CO_2 capture integrated with mechanical vapor recompression technology[J]. Separation and Purification Technology, 2022, 294: 121202.
[18] Austrian Institute of Technology. AHEAD - Advanced Heat Pump Demonstrator. https://www.ait.ac.at/en/ahead.
[19] Feng C, Guo C, Chen J, et al. Theoretical study of an auto-cascade high-temperature heat pump using vapor injection and parallel compression techniques for steam generation[J]. Thermal Science and Engineering Progress, 2025, 60: 103482.
[20] Chen J, Wang D, Zhang G, et al. 4E analyses of a novel solar-assisted vapor injection autocascade high-temperature heat pump based on genetic algorithm[J]. Energy Conversion and Management, 2024, 299: 117863.
[21] Ma D, Sun Y, Ma S, et al. Study on the working medium of high temperature heat pump suitable for industrial waste heat recovery[J]. Applied Thermal Engineering, 2024, 236: 121642.
[22] Adamson K M, Walmsley T G, Carson J K, et al. High-temperature and transcritical heat pump cycles and advancements: A review[J]. Renewable and Sustainable Energy Reviews, 2022, 167: 112798.
[23] Dai B, Liu X, Liu S, et al. Life cycle performance evaluation of cascade-heating high temperature heat pump system for waste heat utilization: Energy consumption, emissions and financial analyses[J]. Energy, 2022, 261: 125314.